



Universiteit
Leiden
The Netherlands

Mini-, micro-, and conventional electrodes an in vivo electrophysiology and ex vivo histology head-to-head comparison

Glashan, C.A.; Beukers, H.K.C.; Tofig, B.J.; Tao, Q.; Blom, S.; Mertens, B.; ... ; Zeppenfeld, K.

Citation

Glashan, C. A., Beukers, H. K. C., Tofig, B. J., Tao, Q., Blom, S., Mertens, B., ... Zeppenfeld, K. (2021). Mini-, micro-, and conventional electrodes an in vivo electrophysiology and ex vivo histology head-to-head comparison. *Jacc: Clinical Electrophysiology*, 7(2), 197-205.
doi:10.1016/j.jacep.2020.08.014

Version: Publisher's Version
License: [Leiden University Non-exclusive license](#)
Downloaded from: <https://hdl.handle.net/1887/3279800>

Note: To cite this publication please use the final published version (if applicable).

CATHETER ABLATION: TECHNOLOGY

Mini-, Micro-, and Conventional Electrodes



An in Vivo Electrophysiology and Ex Vivo Histology Head-to-Head Comparison

Claire A. Glashan, MD,^a Hans K.C. Beukers, MD,^a Bawer J. Tofig, MD, PhD,^b Qian Tao, PhD,^c Sira Blom, BSc,^a Bart Mertens, PhD,^d Steen B. Kristiansen, MD, PhD,^b Katja Zeppenfeld, MD, PhD^a

ABSTRACT

OBJECTIVES This study sought to assess the relative effect of catheter, tissue, and catheter-tissue parameters, on the ability to determine the amount of viable myocardium in vivo.

BACKGROUND Although multiple variables impact bipolar voltages (BVs), electrode size, interelectrode spacing, and directional dependency are of particular interest with the development of catheters incorporating mini and microelectrodes.

METHODS Nine swine with early reperfusion myocardial infarctions were mapped using the QDot catheter and then remapped using a Pentaray catheter. All QDot points were matched with Pentaray points within 5 mm. The swine were sacrificed, and mapping data projected onto the heart. Transmural biopsies corresponding to mapping points were obtained, allowing a comparison of electrograms recorded by mini, micro-, and conventional electrodes with histology.

RESULTS The conventional BV of 2,322 QDot points was 1.9 ± 1.3 mV. The largest of the 3 microelectrode BVs ($BV_{\mu\text{Max}}$) average 4.8 ± 3.1 mV. The difference between the largest ($BV_{\mu\text{Max}}$) and smallest ($BV_{\mu\text{Min}}$) at a given location was $53.7 \pm 18.1\%$. The relationships between both $BV_{\mu\text{Max}}$ and $BV_{\mu\text{Min}}$ and between the conventional BV and $BV_{\mu\text{Max}}$ were positively related but with a significant spread in data, which was more pronounced for the latter. Pentaray points positively related to the $BV_{\mu\text{Max}}$ with poor fit. On histology, increasing viable myocardium increased voltage, but both the slope coefficient and fit were best for $BV_{\mu\text{Max}}$.

CONCLUSIONS Using histology, we could demonstrate that $BV_{\mu\text{Max}}$ is superior to identify viable myocardium compared with BV_c and BV using the Pentaray catheter. The ability to simultaneously record 3 BV_{μ} s with different orientations, for the same beat, with controllable contact and selecting $BV_{\mu\text{Max}}$ for local BV may partially compensate for wave front direction. (J Am Coll Cardiol EP 2021;7:197-205) © 2021 by the American College of Cardiology Foundation.

From the ^aDepartment of Cardiology, Leiden University Medical Center, Leiden, the Netherlands; ^bDepartment of Cardiology, Aarhus University Hospital, Aarhus, Denmark; ^cDivision of Image Processing, Department of Radiology, Leiden University Medical Center, Leiden, the Netherlands; and the ^dDepartment of Biomedical Data Sciences, Leiden University Medical Center, Leiden, the Netherlands.

The authors attest they are in compliance with human studies committees and animal welfare regulations of the authors' institutions and Food and Drug Administration guidelines, including patient consent where appropriate. For more information, visit the [Author Center](#).

Manuscript received April 13, 2020; revised manuscript received August 11, 2020, accepted August 12, 2020.

**ABBREVIATIONS
AND ACRONYMS**

- BV** = bipolar voltage
- BV_μ** = bipolar voltage using micro-electrode on QDot catheter
- BV_{μMax}** = largest of 3 micro-bipolar voltages using micro-electrodes on QDot catheter
- BV_{μMin}** = smallest of 3 micro-bipolar voltages using micro-electrodes on QDot catheter
- BV_C** = bipolar voltage using conventional electrodes on QDot catheter
- BV_P** = bipolar voltage using Pentaray catheter
- EAM** = electroanatomical mapping
- IQR** = interquartile range
- VM** = viable myocardium

Electroanatomical bipolar voltage (BV) mapping has become a pillar of substrate-based ablation for ventricular tachycardias (1). The amplitudes of the BV electrograms collected are used to ascertain information about the tissue being mapped with the underlying assumption that the electrogram amplitude is directly proportional to the amount of viable myocardium (VM) at that location. Although this relationship has been shown to be true (2), the amount of VM (and inversely, the amount of nonconducting tissue such as scar) is not the only parameter to influence BV amplitudes (3). Additional tissue-specific parameters that influence BV include local conduction velocity and gap junction disarray. Catheter-related parameters that effect electrogram characteristics are electrode size and interelectrode spacing. Catheters with small electrodes can record higher voltages and may detect small amounts of VM.

Narrow interelectrode spacing may increase the near-field resolution (4). Furthermore, parameters

related to the interaction between tissue and catheter are of importance. These include the contact force and angle of incidence between catheter and tissue, as well as the relative orientation of the catheter bipole to the activation wave front direction. Simultaneous recordings from orthogonal electrode pairs have shown that the wave front can account for up to a 49% difference in BV amplitude (5).

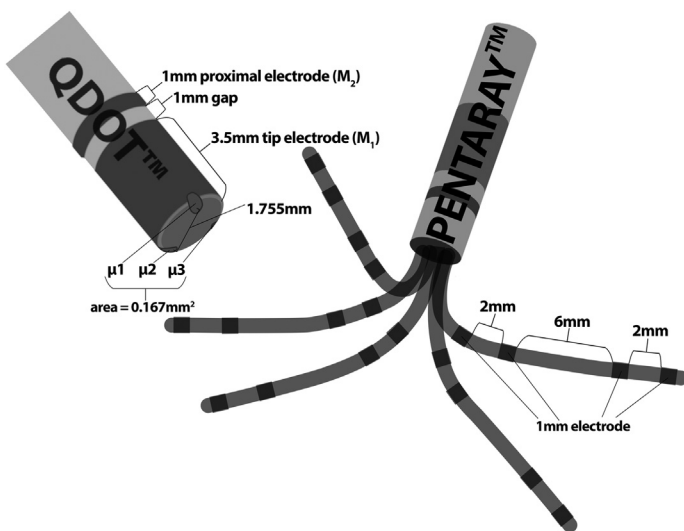
With the development of new catheters incorporating mini and micro-electrodes, there has been much focus on the effect of electrode size and spacing, whereas the interaction between electrode orientation and wave front direction has not been systematically evaluated. To be able to assess the relative effect of catheter and catheter tissue parameters on the ability to determine the amount of VM in vivo, an approach that keeps other parameters constant and uses an undeniable gold-standard is desirable. Here, we perform a head-to-head comparison of voltages generated using the QDot (Biosense Webster, Irvine, California) and Pentaray (Biosense Webster) catheters and the gold standard for scar identification: histology (2,4).

SEE PAGE 206

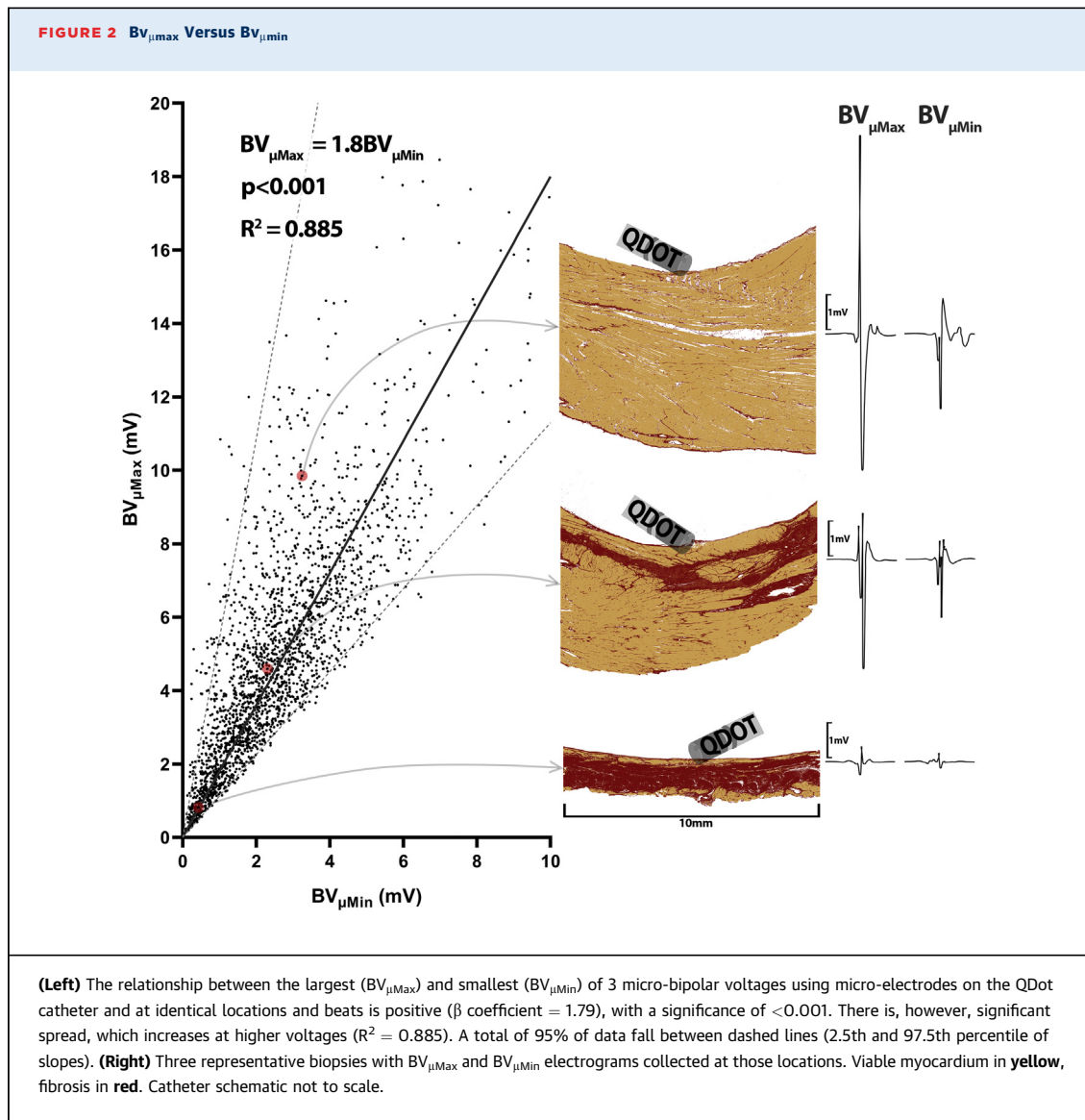
METHODS

ELECTROANATOMICAL MAPPING. The study was approved by the Danish Animal Experiments Inspectorate (jr. nr. 2017-15-0201-01259) and complied with local institutional guidelines. In 9 domestic Danish swine (67 ± 2 kg), a myocardial infarction was induced by inflating an intravascular balloon in the left anterior descending coronary artery (after the second diagonal branch) for 65 min before deflation. This model gives rise to a more patchy scar, including areas of transmural as well as of nontransmural scar, more closely mimicking human reperfusion infarctions than do models using longer occlusion times (4,6). The QDot 3.5-mm-tip electrode integrates 3 micro-electrodes (surface area 0.167 mm^2 , interelectrode distance 1.755 mm, angle between micro-bipoles 60°) recording 3 micro-bipolar electrograms (bipolar voltage using micro-electrode on QDot catheter [BV_μ]). The distal QDot -bipole (3.5-mm tip, 1-mm ring, 1-mm spacing) simultaneously records the conventional BV (BV_C) at a 90° angle to the 3 micro-bipoles. Care was taken to ensure the QDot had an angle of incidence of $<30^\circ$ relative to the left ventricular endocardium and that points were only taken with a contact force of >9 g and at locations with stable amplitudes. The left ventricle was then remapped with a Pentaray catheter. The Pentaray consists of 5 splines each with 4 1-mm wide

FIGURE 1 Schematic of Catheters Used



The QDot catheter (left) consists of a standard 3.5-mm-tip electrode (M₁) separated from a 1-mm wide ring electrode (M₂) by a 1-mm gap. Conventional bipolar electrogram (BV_C) is collected between M₁ and M₂. Integrated in the tip of the catheter are 3 micro-electrodes (μ₁, μ₂, and μ₃), each 0.167 mm^2 in size and separated by 1.755 mm and with an angle of 60° between each of the 3 micro-bipoles. The electrogram collected between the micro-electrodes (BV_μ) is perpendicular to the BV_C bipole. The Pentaray catheter (right) consists of 5 splines, each with 4 1-mm wide electrodes, with a 2-6-2 mm edge-to-edge spacing. Bipolar electrograms (BV_Ps) were collected between each 2-mm-spaced pair.



electrodes (2-6-2 mm edge-to-edge spacing). Bipolar electrograms were collected from each 2-mm spaced pair (BV using Pentaray catheter [BV_P]) (Figure 1). As the Pentaray cannot measure force, care was taken to collect the BV_P point only when the catheter was in a stable position under fluoroscopic visualization to optimize contact and with reproducible near-field electrograms for 3 consecutive beats.

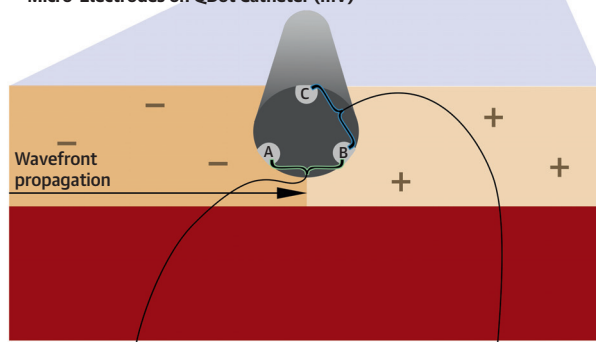
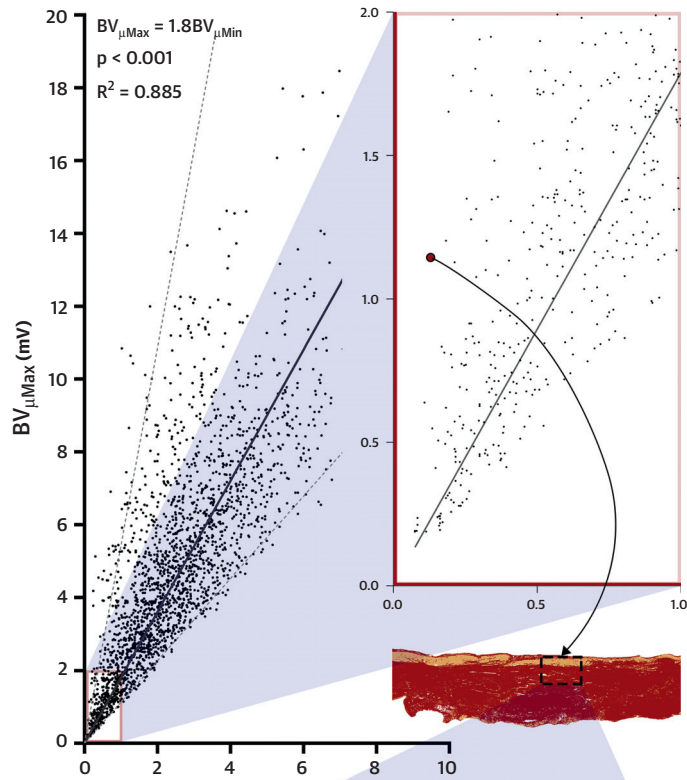
EX VIVO INTEGRATION AND ANALYSIS. After mapping, 3 ablation lesions were placed remotely from the scar as landmarks for accurate image integration. The animals were then sacrificed and processed as previously described (4). In short, the animals were euthanized and the hearts excised and filled with HistOmer (7) to maintain end-diastolic shape. After fixation, the hearts were sliced into 5-mm-thick

slices, and images of these slices were used to create 3-dimensional meshes that were in turn imported into CARTO 3 version 6.0 (Biosense Webster) and merged with electroanatomical mapping (EAM) data.

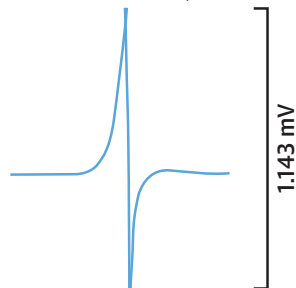
All data were exported and processed in ParaView (v.5.6, Kitware Inc., Clifton Park, New York) with custom-made Python plugins. All EAM points were projected onto the CARTO QDot mesh. For each projected QDot point, the Pentaray point with the largest BV_P within a 5-mm radius was paired and analyzed.

HISTOLOGICAL ANALYSIS. At 196 QDot locations, 10-mm-wide transmural biopsies had been taken and the amount of VM quantified (4). From these, biopsies at locations which had both QDot and Pentaray points were included for this analysis. Areas with $<47 \text{ mm}^2$

CENTRAL ILLUSTRATION Significant Effect of Wavefront Direction on the Amplitude of Bipolar Voltages Collected With Micro-Electrodes

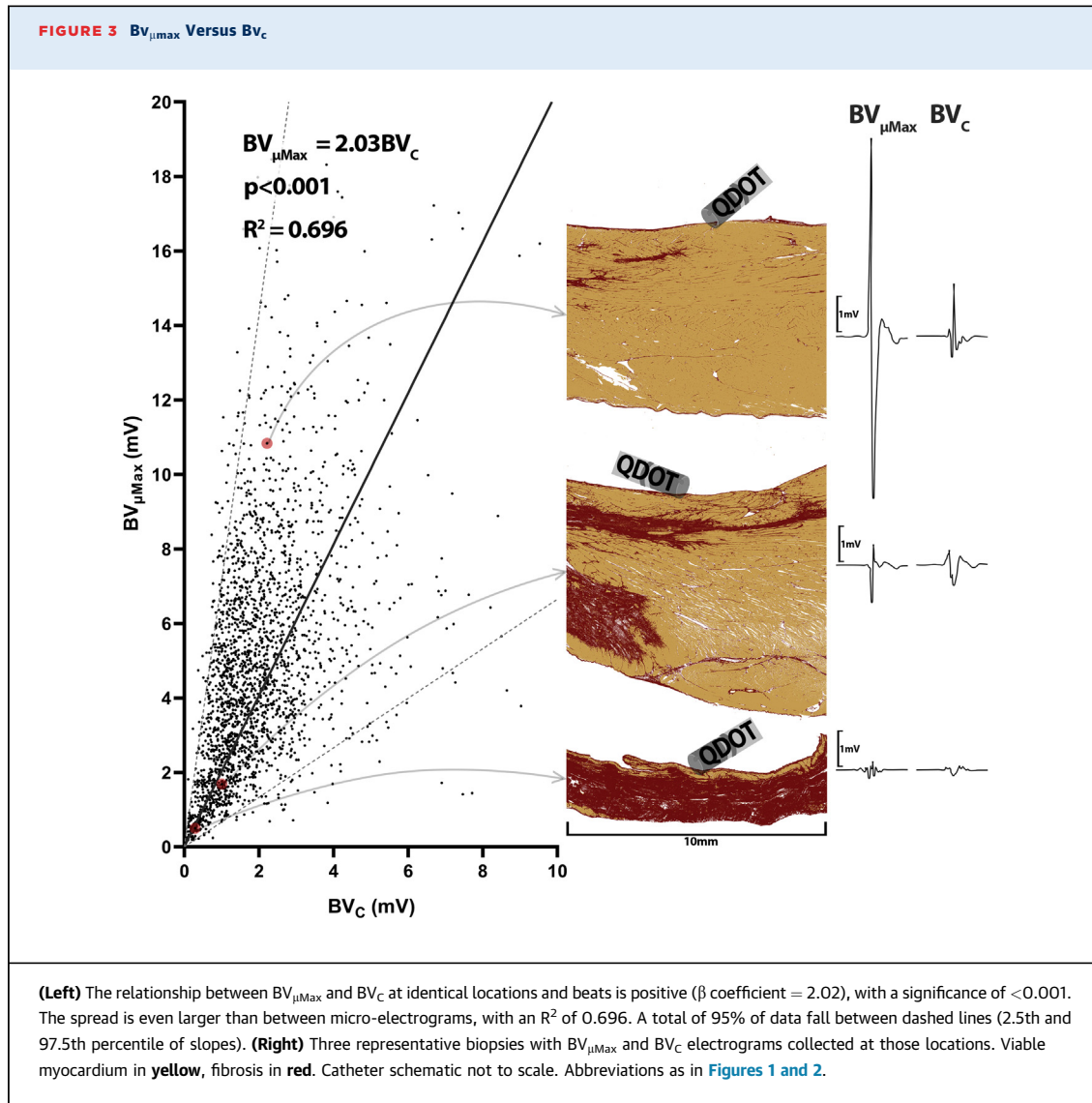


Bipole A-B = $BV_{\mu\text{Max}}$



Bipole C-B = $BV_{\mu\text{Min}}$





VM were considered to have a significant amount of scar (4).

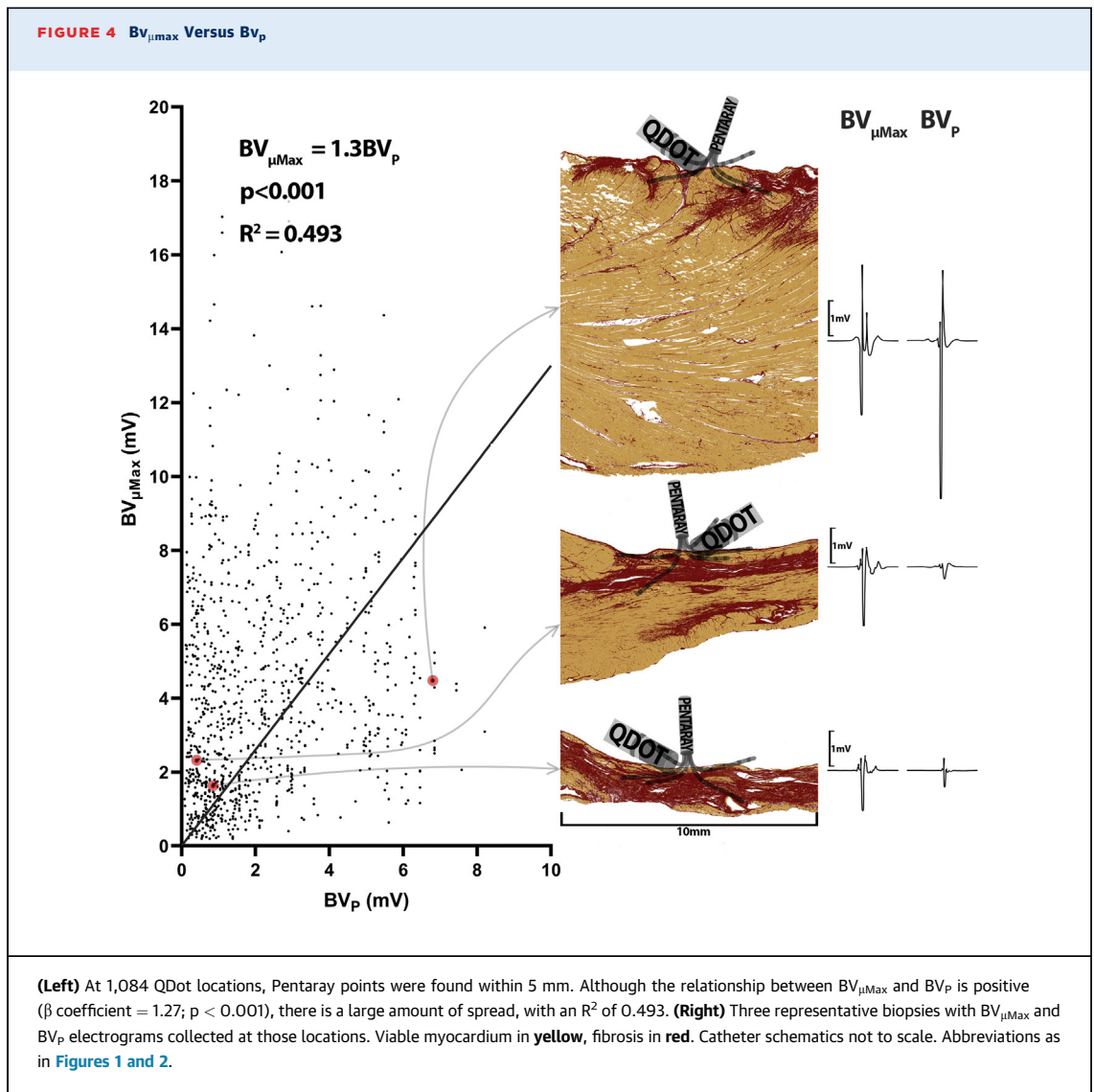
STATISTICAL ANALYSIS. Normally distributed data were reported as mean \pm SD, with non-normally distributed data reported as median (interquartile range [IQR]). As all data were clustered within 9

animals, regression analysis was performed with a bootstrapped mixed effects model.

For data collected from the same catheter, the slope of each point pair collected at the same location was calculated, and the 2.5th and 97.5th percentile of these slopes was determined. Statistical analysis was

CENTRAL ILLUSTRATION Continued

(Top panel) The relationship between the largest ($BV_{\mu\text{Max}}$) and smallest ($BV_{\mu\text{Min}}$) of 3 micro-bipolar voltages using microelectrodes on the QDot catheter at identical locations and beats. The effect of wave front direction, as indicated by the difference in voltage amplitudes ($BV_{\mu\text{Max}}$ vs. $BV_{\mu\text{Min}}$) is large even at low voltages, which may impact detection of thin layer of subendocardial viable tissue if only linear electrode configurations are used (inset top right). **(Bottom panel)** Diagram of a hypothetical situation giving rise to different voltages recorded simultaneously from the 3 bipoles of the QDot. Voltages are generated by a thin layer of viable myocardium (yellow) with wave front propagation from left to right. The amplitude depends on the orientation of bipoles with respect to the traveling wavefront, with the largest amplitude for parallel orientation.



performed using IBM SPSS version 25 (IBM Corporation, Armonk, New York).

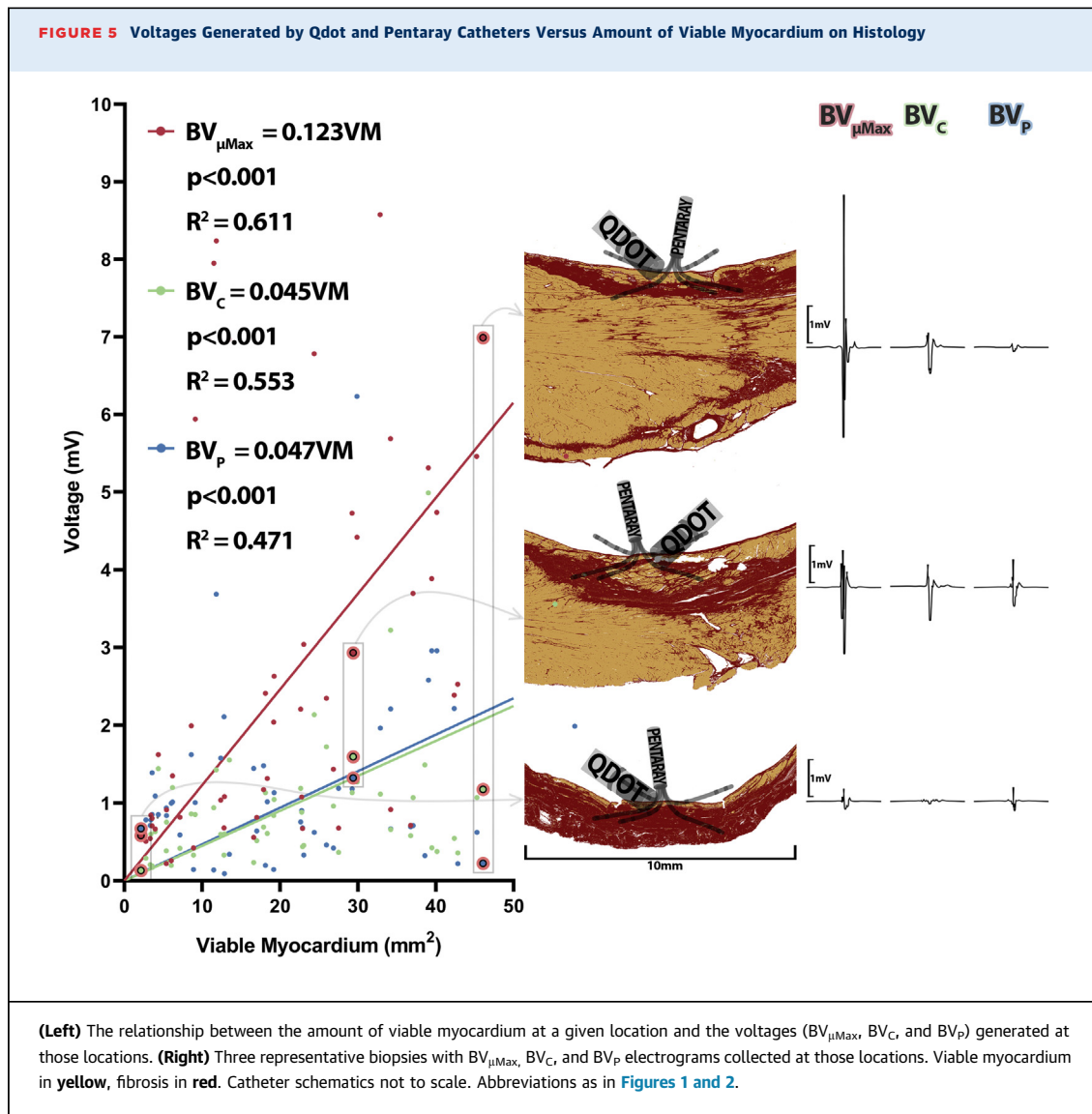
RESULTS

SIMULTANEOUS RECORDINGS OF BV_C AND BV_{μ} . QDot points were collected at 2,322 locations. The BV_C amplitude measured was 1.9 ± 1.3 mV. For every BV_C collected, 3 BV_{μ} s were collected for the exact same beat at the same location. The largest of the 3 ($BV_{\mu\text{Max}}$) averaged 4.8 ± 3.1 mV, and the smallest ($BV_{\mu\text{Min}}$) averaged 2.4 ± 1.7 mV. The difference $BV_{\mu\text{Max}} - BV_{\mu\text{Min}}$ at a given location was 2.3 ± 2.0 mV ($53.7 \pm 18.1\%$). Although there was an overall positive relationship between $BV_{\mu\text{Max}}$ and $BV_{\mu\text{Min}}$ at a given location ($R^2 = 0.885$; $p < 0.001$) (Figure 2), there was an important amount of spread. Differences were more

pronounced at higher voltages, corresponding to higher amounts of VM. However, there were also important differences at low-voltage sites reflecting small subendocardial layers of VM (Central Illustration).

If the amplitude of the $BV_{\mu\text{Max}}$ was compared with the BV_C amplitude, a positive correlation was seen (Figure 3) ($p < 0.001$), with the amplitude of the $BV_{\mu\text{Max}}$ twice that of the BV_C (β coefficient = 2.03). However, the spread in data was even more pronounced, with an R^2 of 0.696.

CONSECUTIVE RECORDINGS OF BV_{μ} AND BV_P . Of all the QDot points, 1,084 were paired with Pentarray points within 5 mm. The mean amplitude of these BV_P points was 2.2 ± 1.9 mV. Although there was a positive relationship ($p < 0.001$) between

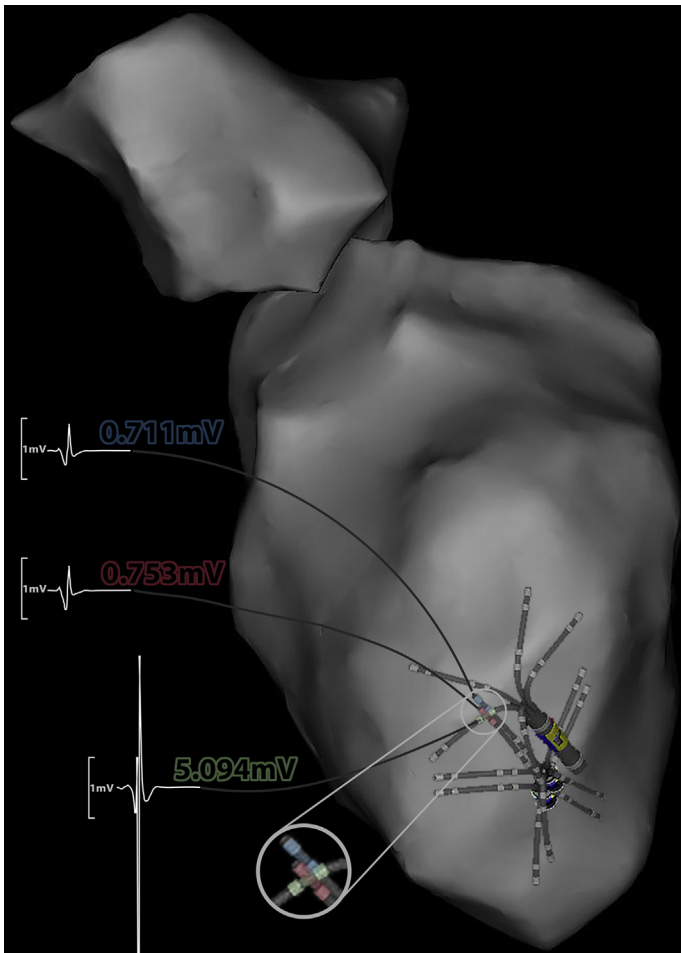


$BV_{\mu\text{Max}}$ and BV_P , the fit was poor ($R^2 = 0.493$) (Figure 4).

COMPARISON OF BV_{μ} , BV_C , AND BV_P WITH AMOUNT OF VM ON HISTOLOGY. Biopsies were taken at 53 scar locations at which both QDot and Pentaray data were available. These biopsies had median wall thickness of 3.6 (IQR: 2.6 to 5.2) mm, 46.6% fibrosis (IQR: 36.5% to 65.0%), and 18.4 (IQR: 8.6 to 29.9) mm² VM. Although all voltages increase with increasing VM ($p < 0.001$ for all), the same increase in VM results in the largest absolute change in $BV_{\mu\text{Max}}$ (β coefficient = 0.123). For a given location, $BV_{\mu\text{Max}}$ showed the best fit between voltage and histology ($R^2 = 0.611$). The poorest fit was seen between VM and BV_P , with an R^2 of 0.471 (Figure 5).

DISCUSSION

Although BV mapping with multiple, smaller, and narrow-spaced electrodes to delineate local VM is considered superior to mapping with large electrodes, the relative impact of different catheter, tissue, and catheter-tissue interaction parameters on BV is unknown (4,8). It has recently been shown that using the largest amplitude of 2 orthogonal pairs of bipoles on a grid catheter leads to smaller scar sizes when using predefined voltage cutoffs (9). Although this suggests the importance of wave front direction, the direct comparison of BV recorded from different electrode pairs at a given location is challenging and its validation by histology lacking.

FIGURE 6 Effect of Wavefront Propagation Direction

Effect of wave front propagation direction on the amplitude of the electrograms generated using the Pentaray catheter at the same location but different bipole orientation.

In our post hoc analysis, comparing $BV_{\mu\text{Max}}$ with $BV_{\mu\text{Min}}$, we were able to control for all parameter but 1: the angle between the 2 bipoles and the activation wave front (Figure 2). As these electrograms were collected at the same location, during the same beat, from the same catheter, tissues parameters were identical. Furthermore, the angle of incidence of the catheter and the contact force between catheter and tissue were also identical. As the 3 microelectrodes on the tip of the QDot catheter have the same size and spacing, these 2 parameters were also controlled for. Nevertheless, we observed a large variation seen between $BV_{\mu\text{Max}}$ and $BV_{\mu\text{Min}}$, suggesting a larger effect of wave front direction on BV amplitude than

previously hypothesized (5,10). Although the difference was larger for higher voltages and corresponding larger amount of VM, there were remarkable inequalities in areas with small amounts of VM. Accordingly, simply reducing electrode size and spacing may not guarantee detection of small areas of subendocardial VM. Detection of these small layers can be improved by simultaneous recordings from different angles with display of the maximum amplitude.

In our second analysis, we introduced 2 additional parameters: electrode size and spacing. Comparing BV_C with $BV_{\mu\text{Max}}$ collected from the same catheter and beat again kept tissue parameters constant and kept the contact force identical. The difference in electrode size and spacing may account for the additional increase in variability illustrated in Figure 3.

Finally, when comparing the voltage collected using the Pentaray with $BV_{\mu\text{Max}}$ collected using the QDot, additional variables need to be considered. Now, not only electrode size, spacing, and activation wavefronts are different, but also because the data were collected using 2 different catheters during remapping, data are being collected during different beats. Although we tried to control for location by only pairing points within 5 mm from each other, even a slight difference in catheter position may have an effect. Another factor that may contribute to the variation seen in Figure 4 is the difference in contact. As the Pentaray cannot measure contact force, the effects of variable spline contact should not be missed. However, the effect of wave front direction remains a potentially large variable, as illustrated in Figure 6. Here, we see an example of 3 Pentaray positions, 2 in which the bipole is the same orientation (highlighted in blue and red)—leading to very similar electrograms. In the third position (green), while the bipole is in almost exactly the same position, it is perpendicular to the first 2 bipoles, and the electrogram amplitude is astonishingly different. The significant bipole orientation dependency (together with electrode size and spacing) may be particularly important for remapping if different catheters for substrate analysis and ablation are used.

STUDY LIMITATIONS. This study was performed post hoc and, as such, some data are limited. This is particularly true with regard to the number of biopsies included in the analysis. Furthermore, we matched QDot points with Pentaray points within a radius of 5 mm. Although small, even this difference in location may have significant effect on the histological substrate underneath the catheter and as such on the voltages generated.

CONCLUSIONS

Using histology as the gold standard, we could demonstrate that $BV_{\mu\text{Max}}$ is superior to identify VM compared with BV_C and BV_P . The ability to simultaneously record 3 BV_{μ} s with different orientations, from the same beat with controllable and stable contact, and selecting $BV_{\mu\text{Max}}$ for local BV may at least partly compensate for wave front direction. A disadvantage of this catheter design is the time required to achieve a high mapping density, which may be mitigated by using image-integration to focus on areas of interest.

FUNDING SUPPORT AND AUTHOR DISCLOSURES

This study was partially supported by an investigator-initiated grant from Biosense Webster (a Johnson and Johnson company). Dr. Tofig was supported by the Arvid Nilssons Foundation. All other authors have reported that they have no relationships relevant to the contents of this paper to disclose.

ADDRESS FOR CORRESPONDENCE: Dr. Katja Zeppenfeld, Leiden University Medical Center, Department of Cardiology (C-05-P), P.O. Box 9600, 2300 RC Leiden, the Netherlands. E-mail: k.zeppenfeld@lumc.nl.

PERSPECTIVES

COMPETENCY IN MEDICAL KNOWLEDGE: Mapping using a multielectrode catheter incorporating microelectrodes allows for partial compensation of wave front direction and better identification of underlying VM.

TRANSLATIONAL OUTLOOK: Further studies in humans are needed to validate the voltage amplitudes generated in this swine model.

REFERENCES

1. Wroblewski D, Houghtaling C, Josephson ME, Ruskin JN, Reddy VY. Use of electrogram characteristics during sinus rhythm to delineate the endocardial scar in a porcine model of healed myocardial infarction. *J Cardiovasc Electrophysiol* 2003;14:524-9.
2. Glashan CA, Androulakis AFA, Tao Q, et al. Whole human heart histology to validate electro-anatomical voltage mapping in patients with non-ischaemic cardiomyopathy and ventricular tachycardia. *Eur Heart J* 2018;39:2867-75.
3. Josephson ME, Anter E. Substrate mapping for ventricular tachycardia: assumptions and misconceptions. *J Am Coll Cardiol EP* 2015;1:341-52.
4. Glashan CA, Tofig BJ, Tao Q, et al. Multisite electrodes for substrate identification in ischemic cardiomyopathy. *J Am Coll Cardiol EP* 2019;5:1130-40.
5. Takigawa M, Relan J, Martin R, et al. Effect of bipolar electrode orientation on local electrogram properties. *Heart Rhythm* 2018;15:1853-61.
6. Wijnmaalen AP, Schalijs MJ, von der Thülen JH, Klautz RJ, Zeppenfeld K. Early reperfusion during acute myocardial infarction affects ventricular tachycardia characteristics and the chronic electroanatomic and histological substrate. *Circulation* 2010;121:1887-95.
7. Bjarkam CR, Pedersen M, Sorensen JC. New strategies for embedding, orientation and sectioning of small brain specimens enable direct correlation to MR-images, brain atlases, or use of unbiased stereology. *J Neurosci Methods* 2001;108:153-9.
8. Leshem E, Tschabrunn CM, Jang J, et al. High-resolution mapping of ventricular scar: evaluation of a novel integrated multielectrode mapping and ablation catheter. *J Am Coll Cardiol EP* 2017;3:220-31.
9. Jiang R, Beaser AD, Aziz Z, Upadhyay GA, Nayak HM, Tung R. High-density grid catheter for detailed mapping of sinus rhythm and scar-related ventricular tachycardia: comparison with a linear duodecapolar catheter. *J Am Coll Cardiol EP* 2020;6:311-23.
10. Porta-Sanchez A, Magtibay K, Nayyar S, et al. Omnipolarity applied to equi-spaced electrode array for ventricular tachycardia substrate mapping. *Europace* 2019;21:813-21.

KEY WORDS electrode size, electrode spacing, histology, microelectrodes, mini electrodes, swine, voltage mapping